Effect of Seed Layer Thickness on Texture and Electrical Properties of Sol−Gel Derived (Ba 0.8 Sr 0.2)TiO 3 Thin Films

3 AUTHORS, INCLUDING:

Paula Vilarinho
University of Aveiro

317 PUBLICATIONS **3,448** CITATIONS

Effect of Seed Layer Thickness on Texture and Electrical Properties of Sol−Gel Derived (Ba$_{0.8}$Sr$_{0.2}$)TiO$_3$ Thin Films

Zhi Fu, Aiying Wu, and Paula M. Vilarinho*

Department of Ceramics and Glass Engineering, CICECO, University of Aveiro,
3810-193 Aveiro, Portugal

The perovskite phase nucleation and growth of Ba$_{0.8}$Sr$_{0.2}$TiO$_3$ [BST(80/20)] films was restricted to the bottom interface by the use of a Ba$_{0.8}$Sr$_{0.2}$TiO$_3$ [BST(80/20)] sol−gel seed layer of optimized thickness. As a result (h00) preferred orientation, BST thin films on Pt/Ti/SiO$_2$/Si with enhanced electric properties were prepared by sol−gel at considerably low temperatures (700 °C). The effect of sol−gel seed layers and their thickness on the structure/microstructure and electric properties of BST sol−gel derived films was evaluated in this study. 400-nm-thick BST films with a 30-nm-thick seed layer showed a maximized (h00) preferred orientation growth with a grain size of 120 nm. The dielectric constant varied from 300 to 830 at 1 kHz and from 230 to 580 at 1 MHz for films without a seed layer and with a 30-nm-thick seed layer, respectively. In addition the tunability of the dielectric constant was improved to ∼37% at 150 kV/cm, compared with that without seed layer. The remanant polarization and leakage current of BST films with an optimal seed layer were 1.6 μC/cm^2 with a coercive field of 30 kV/cm and 8.0 × 10^{-7} A/cm^2 up to an applied electric field of 167.5 kV/cm, respectively. The electrical performance of these BST films is discussed in relation to the effect of the seed layer thickness on the texture and microstructure of the films.

1. Introduction

(Ba$_{1-x}$Sr$_x$)TiO$_3$ (BST) ferroelectric thin films possess exceptional dielectric properties (high dielectric constant, relatively low loss, and fast switching speed), over a wide frequency range (up to >1 GHz), and large electric-field dielectric tunability.[1] These features make BST thin films technology attractive for high-density dynamic random access memories, DRAMs,[2] and to low cost agile microwave circuits, such as phase shifters, tunable filters, tunable matching network, and high tuning frequency range voltage controlled oscillators.[3] High-density BST multilayer capacitor technology presents unique miniaturization advantages for various electronic modules and packages. By utilizing BST capacitors with a wide range (0.5 pF to 500 nF), functions such as decoupling, bypassing, and varying capacitance (voltage tunable) can be realized with a single thin-film passive chip.[4] According to Gennum Corp., such miniaturized multi-functional capacitor chips can improve the performance and reduce the size of multi-chip modules and Systems-in-Package.[4] BST as a candidate for very compact monolithic microwave integrated circuit decoupling capacitors promises a 100-fold reduction in capacitor area as compared with SiN and SiO$_2$ capacitors.[1]

The dielectric properties and dielectric tuning property of BST thin films are closely related to the film composition, substrate type, and post-deposition process. It is well-known that the electrode−film interface, stress state, microstructure, texture, and surface morphology markedly affect the electric response of BST films.[5] It has been reported that the evolution of the microstructure of thin films during heat treatment is affected by the process of deposition (physical or chemical solution deposition) and process variables, by the nature of the substrate, the film thickness, and the heat treatment cycle.[6] As a result of the anisotropic dielectric properties of BST films, researchers recently have been focused on the investigation of crystallographic orientated growth of BST films to maximize the dielectric response.[7] A range of methods to obtain textured BST films, such as the control of heat treatment conditions,[8] the insertion of seed layers (or intermediate layers),[9,10] and/or the choice of different bottom electrodes,[11] have been reported.

* Corresponding author. Tel.: 351 234 370354/259. Fax: 351 234 425300. E-mail: paulas@cv.ua.pt.

(1) Zhu, X.; Zhu, J.; Zhou, S.; Liu, Z.; Ming, N.; Lu, S.; Chan, H. L.-W.; Choy, C.-L. *J. Electron. Mater.* **2003**, *32*, 10, 1125.

(2) Baniecki, J. D.; Laibowitz, R. B.; Shaw, T. M.; Duncombe, P. R.; Neumayer, D. A.; Kotecki, D. E.; Shen, H.; Ma, Q. Y. *Appl. Phys. Lett.* **1998**, *72*, 498−500.

(3) Xu, H.; Pervez, N. K.; Park, J.; Sanabria, C.; York, R. A. Presented at 17th International Symposium on Integrated Ferroelectrics, Shanghai, China, April 2005.

(4) Gennum Corp. Home Page. www.gennum.com/technology/ (accessed Feb 2005).

(5) Streiffer, S. K.; Basceri, C.; Parker, C. B.; Lash, S. E.; Kingon, A. I. *J. Appl. Phys.* **1999**, *86*, 4565−4575.

(6) Schwartz, R. W.; Clem, P. G.; Voigt, J. A.; Byhoff, E. R.; Stry, M. V.; Headley, T. J.; Missert, N. A. *J. Am. Ceram. Soc.* **1999**, *82*, 2359−2367.

(7) Moon, S. E.; Kim, E.-K.; Kwark, M.-H.; Ryu, H.-C.; Kim, Y.-T.; Kang, K.-Y.; Lee, S.-J.; Kim, W.-J. *Appl. Phys. Lett.* **2003**, *83*, 2166−2168.

(8) Hwang, C. S.; Joo, S. H. *J. Appl. Phys.* **1999**, *85*, 2431−2436.

(9) Park, B. H.; Peterson, E. J.; Jia, Q. X. *Appl. Phys. Lett.* **2001**, *78*, 533−535.

(10) Jeon, Y.-A.; Shin, W.-C.; Seo, T.-S.; Yoon, S.-G. *J. Mater. Res.* **2002**, *17*, 2831−2836.

(11) Majumder, S. B.; Jain, M.; Martinez, A.; Katiyar, R. S. *J. Appl. Phys.* **2001**, *90*, 896−903.

Majumder et al.[11] prepared (100) textured BST(50/50) films with an enhanced dielectric constant of 1500 on $SrTiO_3$ (ST) and $LaAlO_3$ (LAO) substrates by sol−gel after annealing at 1100 °C for 6 h. Jeon et al.[10,12] investigated $(Ba_{0.5}Sr_{0.5})TiO_3$ thin films prepared by pulsed laser deposition (PLD) and metal organic chemical vapor deposition on a $Pt/Ti/SiO_2/Si$ substrate with BST and $(Ba,Sr)RuO_3$ (BSR) seed layers. The authors reported a (100) preferred orientation of BST films with dielectric constants of 720 and 1300 at 100 kHz for the BST and BSR seed layers, respectively. Dawley and Clem[13] reported (100) enhanced orientation of $(Ba_xSr_{1−x})TiO_3$ ($x = 0.33$, 0.5 and 0.67) films with dielectric constant values of 980−1500 at 100 kHz prepared by chemical solution deposition (CSD) on $Pt/Ti/SiO_2/Si$ with a Ni buffer layer and annealed at 900 °C in a reducing atmosphere.

As a result of film growth mechanisms, vacuum deposition techniques, such as PLD and radio frequency magnetron sputtering, among others, are the most adequate to prepare oriented films, and consequently, epitaxial or textured grown films are relatively easy to be obtained through these methods.[11,14,15] Alternatively, CSD techniques, such as sol−gel, are quite attractive because they provide easy control of the stoichiometry (fundamental for ferroelectric related functional oxides), high chemical purity, high chemical and microstructural homogeneity, possibility of large area deposition, low equipment cost, and a uniformity of the thickness of the deposited films. However, it is difficult for films fabricated by sol−gel to grow according to a preferred orientation, because the nucleation events are equally probable throughout the bulk of the film as in the film−substrate interface, and nucleation through the bulk of the film results in a polycrystalline film. In other words, if preferred orientation of BST films is required, the nucleation events must be limited to the film−substrate interface, which is hard to control by the sol−gel method, especially at low temperature on the $Pt/Ti/SiO_2/Si$ substrate.

Most previous works covered the preparation of textured BST films by vacuum techniques. Few works report the use of solution deposition to prepare highly orientated BST films. And from these, in which the reported annealing temperatures are high, it was observed that BST films with enhanced crystallographic orientation show superior dielectric properties.[7−10] However, the effect of the thickness of the seed layer has not been systematically addressed in the preparation of BST films.

In the present work, sol−gel derived ($h00$) orientated BST-(80/20) thin films were prepared at low annealing temperatures, 700 °C, on the $Pt/Ti/SiO_2/Si$ substrate through the use of BST seed layers also prepared by the sol−gel process. The effect of the seed layer thickness on the texture degree and final electrical properties of BST thin films was studied. X-ray diffraction (XRD) and scanning electron microscopy (SEM) analysis were used to evaluate the texture, micro-

structure, and morphology of the films. The dielectric constant and loss tangent, leakage current, tunability, and remanant polarization were measured. The correlation between the orientation and the dielectric properties is established and discussed.

2. Experimental Details

$Ba_{0.8}Sr_{0.2}TiO_3$ [BST(80/20)] thin films with and without seed layers on $Pt/Ti/SiO_2/Si$ substrate were prepared by a modified sol−gel method. $Ba(CH_3COO)_2$ (Merck, 99%), $Sr(CH_3COO)_2 \cdot {}^1/_2H_2O$ (ABCR, 98%), and $Ti(OC_4H_9)_4$ (Merck, >98%) were used as starting materials. Glacial acetic acid (CH_3COOH, Merck, >99.8%) and ethylene glycol ($HOCH_2CH_2OH$, Merck, >99.5%) were used as the solvent, and acetylacetone ($C_5H_8O_2$, Merck, >99.5%) was used as the stabilizer for Ti alkoxide. $Ba(CH_3COO)_2$ and $Sr(CH_3COO)_2 \cdot {}^1/_2H_2O$ powders with a molar ratio of 8:2 were dissolved in acetic acid and heated to 80 °C under constant stirring. $Ti(OC_4H_9)_4$ was stabilized with a mixture of ethylene glycol and acetylacetone. The stabilized $Ti(OC_4H_9)_4$ solution was mixed with $Ba(CH_3COO)_2/Sr(CH_3COO)_2$ solution with a molar ratio of 1:1 under constant stirring. After stirring for 2 h, the solution concentration was adjusted to 0.25 mol/L and stirred for 1 h more. For the fabrication of the seed layers, the precursor solution was deposited by spin-coating at 4000 rpm for 30 s on $Pt/Ti/SiO_2/Si$ substrates, which were ultrasonically cleaned in acetone and ethanol solvent, respectively. The as-deposited seed layer was dried in air at 150 °C for 5 min and pyrolyzed at 350 °C for 5 min on a hot plate. Seed layers with different thicknesses (15, 30, and 45 nm) were obtained by repeating the deposition−heating process. Finally the seed layer was annealed at 600 °C for 1 h by directly inserting the coated substrate into a tube furnace at the desired temperature. $(Ba_{0.8}Sr_{0.2})TiO_3$ films were prepared by spinning the precursor solution at 3000 rpm for 30 s onto uncoated or coated with seed layers $Pt/Ti/SiO_2/Si$ substrates. Each as-deposited film layer was dried at 150 °C for 5 min and pyrolyzed at 350 °C for 5 min. The total thickness of the BST films was obtained by repeating the described process. At last, BST films with and without seed layers were annealed at 700 °C for 1 h. The final thickness of the BST films, including seed layers, was approximately 400 nm for all the films as determined by SEM.

The phase evolution, degree of orientation, microstructure, grain morphology, and thickness of BST seed layers and BST films were characterized using XRD (Rigaku, Geigerflex D/Max-C series, and Philips XPert MRD diffractometer) and SEM (Hitachi, S-4100). X-ray rocking curves were obtained by tilting the BST films through the Bragg angle of the (200) plane. The X-ray pole figure measurements were performed with a Philips XPert MRD diffractometer, using a Cu Kα X-ray source with a crossed slit incident optic and open receiving slit of 1 mm before the proportional detector. The samples were rotated 180° about the cp axis (azimuthal rotation) and 90° about the yr axis (tilt). In the pole figure measurements the diffracted intensity was collected at a step of 5° in the tilting and rotating angles in the whole hemisphere, at a fixed $\theta−2\theta$ angle of the open detector, that corresponds to the (101) and (200) reflections of BST films while the specimen was tilted and azimuthally rotated in relation to the incident beam. The partial pole figures are plotted. For the evaluation of electrical properties, metal−insulator−metal (MIM) capacitors with Pt/BST/Au structures were fabricated. The Au top circular electrodes were sputtered using a shadow mask. Then BST films with top electrodes were post-annealed at 200 °C for 30 min to improve the interface between the metal and the films. The dielectric constant and loss tangent were evaluated with an impedance bridge (HP 4284A) over a

(12) Jeon, Y.-A.; Shin, W.-C.; Seo, T.-S.; Yoon, S.-G. *Appl. Phys. Lett.* **2001**, *79*, 1012−1014.
(13) Dawley, J. T.; Clem, P. G. *Appl. Phys. Lett.* **2002**, *81*, 3028−3030.
(14) Shaw, T. M.; Suo, Z.; Huang, M.; Liniger, E.; Laibowitz, R. B.; Baniecki, J. D. *Appl. Phys. Lett.* **1999**, *75*, 2129−2131.
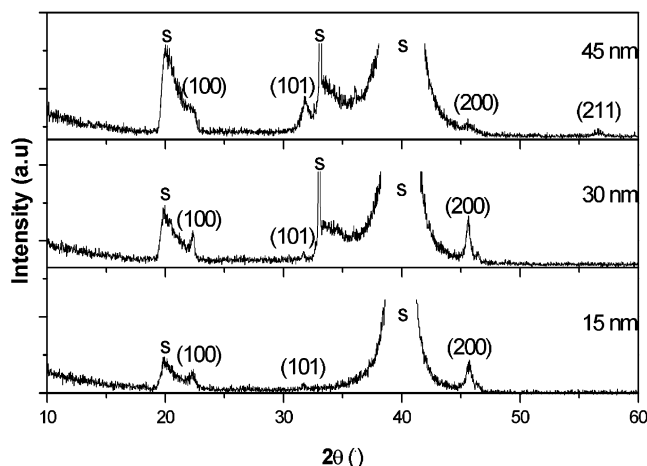(15) Shin, J. C.; Ark, J.; Hwang, C. S.; Kim, H. J. *J. Appl. Phys.* **1999**, *86*, 506−513.

Figure 1. XRD profiles of $(Ba_{0.8}Sr_{0.2})TiO_3$ seed layers with thicknesses of 15, 30, and 45 nm, annealed at 600 °C (S = substrate).
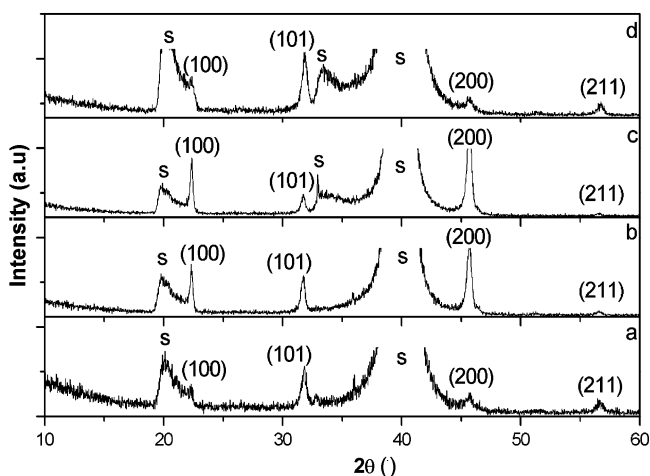

Figure 2. XRD profiles of $(Ba_{0.8}Sr_{0.2})TiO_3$ films annealed at 700 °C with (a) 0, (b) 15, (c) 30, and (d) 45 nm thick seed layers (S = substrate).

frequency range of 100 Hz to 1 MHz. The oscillation level of the applied voltage was set to 0.2 V. The direct current (dc) electric field dependence of the dielectric constant at room temperature (25 °C) was measured to evaluate the tunability of the BST thin films. The measurements were conducted by applying a small alternating current (ac) signal of 0.2 V amplitude and 100 kHz frequency (HP4284 impedance analyzer) while the dc bias was swept from positive voltage to negative voltage and back to positive voltage to check for any possible hysteretic behavior. The current−voltage characteristics of MIM devices were measured using a KEITHLEY 617 programmable electrometer. The polarization behavior of BST thin films was measured by recording the ferroelectric hysteresis loops using an AixACT TF analyzer as a function of the seed layer thickness.

3. Results

Figure 1 shows the XRD patterns of the seed layers annealed at 600 °C for 1 h. Pure $(Ba_{0.8}Sr_{0.2})TiO_3$ perovskite phase was obtained for the different seed layers. The XRD patterns of Figure 1 also clearly indicate that seed layers with thickness equal or inferior to 30 nm have a (h00) preferred orientation, while thicker seed layers (45 nm) show a polycrystalline pattern without any preferred orientation (the thickness of seed layer was determined by SEM).

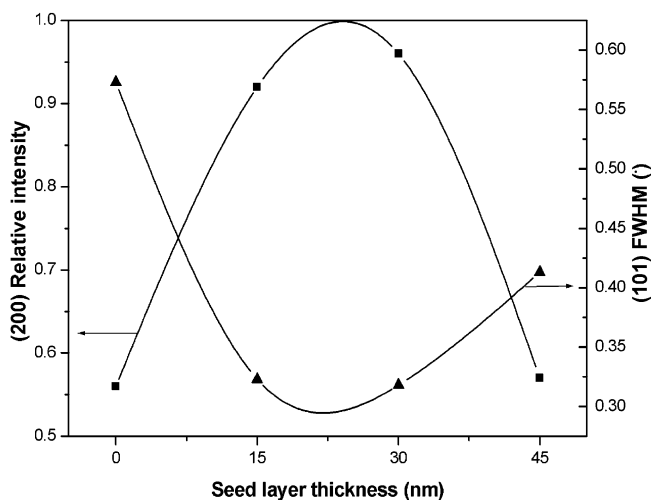Figure 2 illustrates the XRD patterns of different BST films annealed at 700 °C. All the films consist of the pure

Figure 3. Variation of relative intensity of (200) peak and FWHM of the (101) peak of $(Ba_{0.8}Sr_{0.2})TiO_3$ films as a function of the seed layers thickness.

perovskite phase, independently of the presence or thickness of the seed layer. BST films without seed layer showed a polycrystalline random pattern with a (101) predominant peak (Figure 2a). In contrast, BST films with seed layers (≤30 nm thickness) exhibited a (h00) preferred orientation (Figure 2b,c). As shown in Figure 2, the (h00) peak intensity of the BST films was considerably enhanced as the thickness of the seed layer increased up to 30 nm. However, when the seed layer thickness was further increased to 45 nm, the BST film lost the (h00) preferred orientation (Figure 2d), in a manner similar to that of the seed layers themselves (Figure 1). At the same time for identical preparation conditions, films with seed layers exhibit a higher degree of crystallinity than unseeded ones.

The changes on the texture degree and crystallinity resulting from the introduction of seed layers and its dependence on seed layer thickness are clearly illustrated in Figure 3. The relative intensity of the (200) peak and the variation of the full width at half-maximum (FWHM) of the (101) peak were quantitatively estimated as a function of seed layer thickness. The relative intensity of the (200) peak was calculated as

$$I_{(200)} \, [\%] = I_{(200)}/[I_{(200)} + I_{(211)}] \tag{1}$$

where $I_{(hkl)}$ stands for the intensity of (hkl) peaks in $\theta-2\theta$ scans. It is clear from Figure 3 that the FWHM of the (101) peak was remarkably decreased with the insertion of the appropriate seed layer. Meanwhile, the relative intensity of (200) diffraction peaks was rapidly increased from 56% to 95% with the insertion of seed layers and with the increase of seed layer thickness, followed by the decrease to 57% as the thickness of the seed layer was further augmented.

To better analyze the preferred (h00) orientation of BST films due to the insertion of seed layers indicated in the previous analysis, XRD rocking curves and pole figures were conducted and are illustrated in Figures 4 and 5, respectively.

As evidently shown in the rocking curves of Figure 4, a relatively intense and narrow peak is displayed for BST films with 15 and 30 nm thick seed layers when compared to the less intense and broadened peak of those without and with
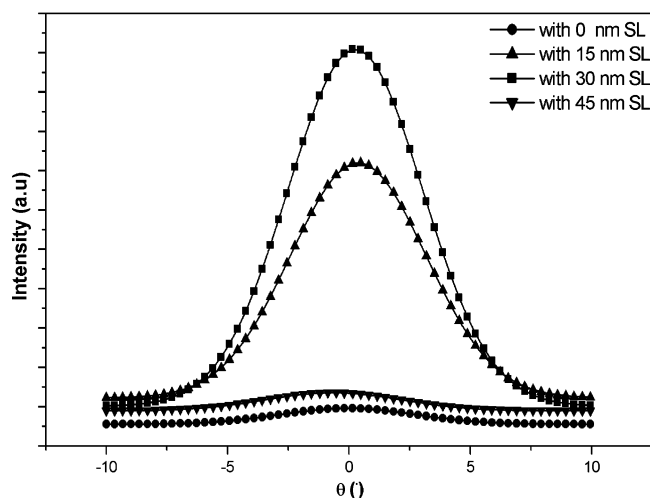
Figure 4. Rocking curves of (200) peak of $(Ba_{0.8}Sr_{0.2})TiO_3$ films with 0, 15, 30, and 45 nm thick seed layers (SL = seed layer).

45 nm thick seed layers. The ratio of the FWHM of the (200) peak to the corresponding intensity calculated from the rocking curve is 0.01°/count and 0.02°/count for the BST films with 30 and 15 nm thick seed layers and 0.19°/count and 0.15°/count for BST films without and with 45 nm thick seed layer, respectively. These results are consistent with the XRD patterns shown in Figure 2.

The texture of the films with a 30 nm thick seed layer was further examined by the Pole figures method. Figure 5 depicts the X-ray Pole figure distribution corresponding to (101) ($2\theta = 32°$) and (200) ($2\theta = 46°$) diffraction reflections of BST films. The concentration of the piercings grouped together in tight bands in the pole figure for the (200) reflection clearly indicates a stronger texture in this direction when compared with the pole figure for the (101) reflection in which the concentration of the piercings grouped in spread bands shows a weaker texture in this direction, confirming the (h00) preferred orientation of seeded films.

The microstructure of the 45 nm thick seed layer is shown in the SEM micrographs of Figure 6. The microstructure is characterized by a fine-grained uniform structure with a visible random grain growth, typical of a bulk nucleation. The microstructure of BST films deposited on the top of the various seeded layers is depicted in Figure 7. SEM plane-view and cross-sectional images of BST films show that crack-free films with spherical fine grains were obtained. The average grain size was gradually increased from 70 to 100 and to 120 nm as the thickness of the seed layer increased from 0 to 30 nm.

The above obtained results show that the presence and the thickness of a seed layer markedly changed the micro-structure and texture of BST sol−gel films deposited on the
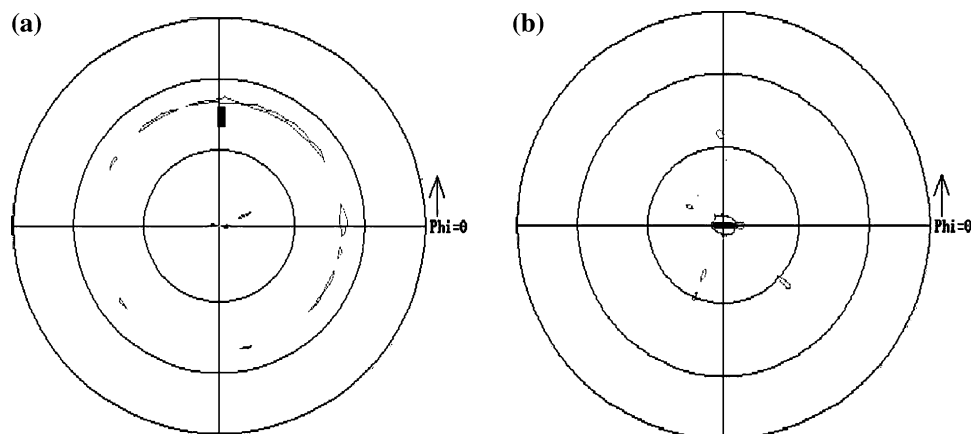

Figure 5. X-ray Pole figure distribution corresponding to (a) (101) ($2\theta = 32°$) and (b) (200) ($2\theta = 46°$) diffraction reflections of BST films with a 30 nm thick seed layer.
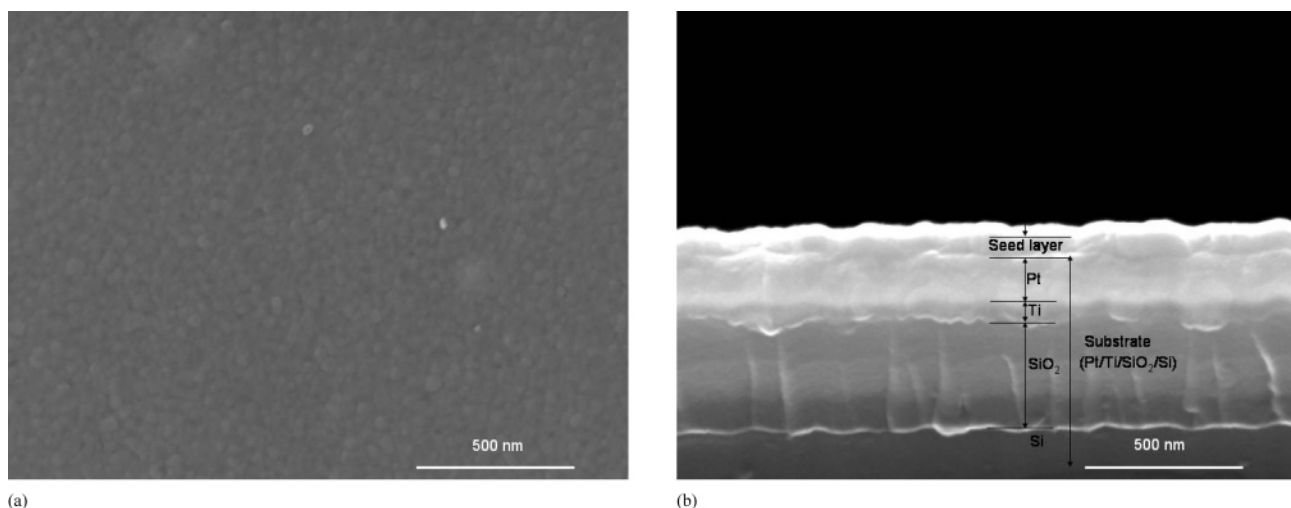

Figure 6. SEM (a) plane-view and (b) cross-sectional images of a 45 nm thick BST seed layer.
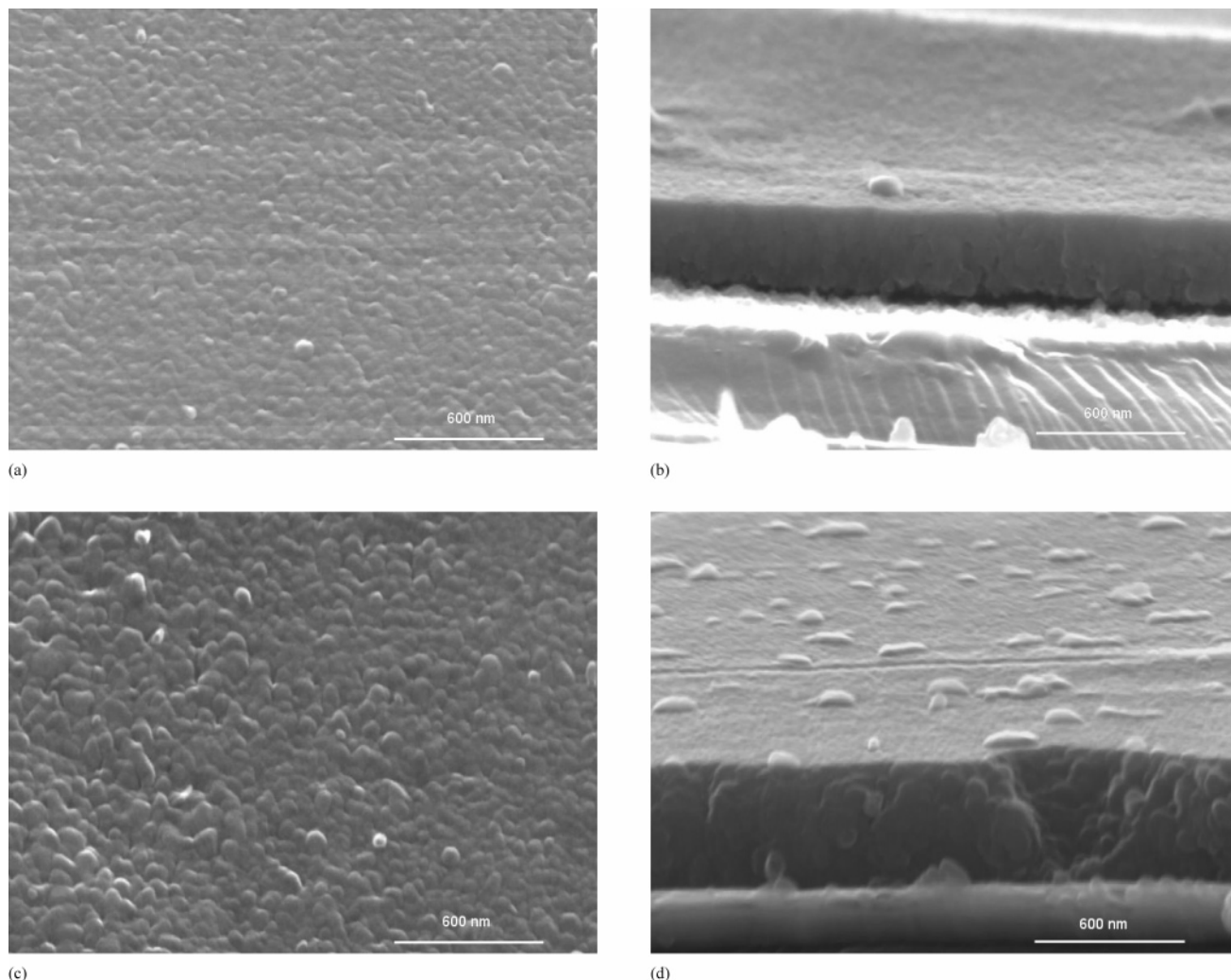
Figure 7. SEM (a and c) plane-view and (b and d) cross-sectional images of (Ba$_{0.8}$Sr$_{0.2}$)TiO$_3$ films without (a and b) and with (c and d) 30 nm thick seed layers.

top of proper thickness seed layers. A maximized (h00) orientation was favored for the 30-nm-thick seed layer. It is now necessary to evaluate this influence on the electrical response.

The effect of seed layers on the electric response of BST films is illustrated in Figures 8−11. As exhibited in Figure 8, the dielectric constant ϵ_r of BST films was enhanced with the insertion of the 15 nm thick seed layer from 250 to 320 at 1 kHz and from 230 to 300 at 1 MHz. A marked enhancement to 830 at 1 kHz and to 580 at 1 MHz was observed when the seed layer thickness was increased to 30 nm. On the other hand, the dielectric losses were not considerably altered by the insertion of seed layers (tan δ = 0.03, 0.04, and 0.05 at 100 kHz, for no seed layer, and 15 and 30 nm thick seed layers, respectively).

The potential of the BST films to be used in voltage-tunable devices depends on the ability to change the dielectric constant and, therefore, capacitance by means of an applied electric field. The dependence of the dielectric constant on the electric field, an indication of the tunability, for BST films at room temperature with and without seed layers, is shown in Figure 9. The relative tunability is defined as the change in the dielectric constant [$\Delta\epsilon_r/\epsilon_r(0)$] induced by a dc
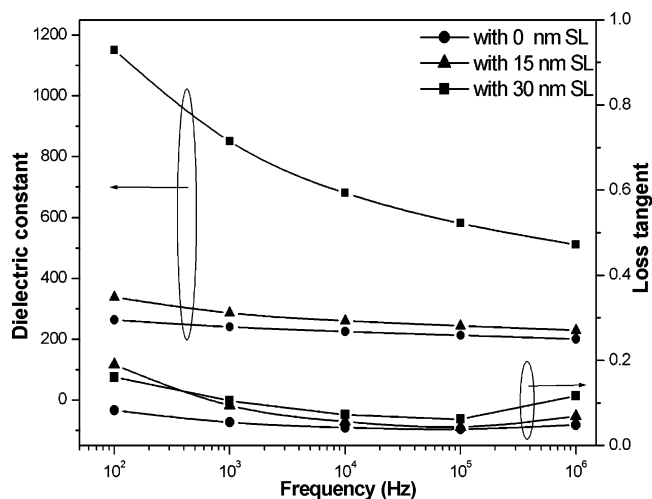

Figure 8. Room-temperature dielectric constant and loss tangent of (Ba$_{0.8}$-Sr$_{0.2}$)TiO$_3$ films with 0, 15, and 30 nm thick seed layers as a function of frequency (SL = seed layer).

field, where $\Delta\epsilon_r$ is the change relative to the zero-bias dielectric constant $\epsilon_r(0)$. The insertion of a 30 nm thick seed layer improved the tunability of BST films and an increment from ~17% to ~37% at 150 kV/cm was observed for unseeded and seeded films. This value is close to that of the
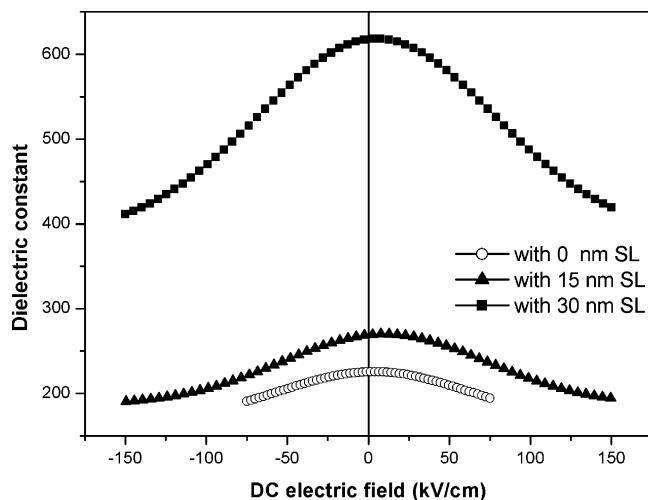
Figure 9. Room-temperature dielectric constant versus dc electric field variation of $(Ba_{0.8}Sr_{0.2})TiO_3$ films with 0, 15, and 30 nm thick seed layers at room temperature (SL = seed layer).
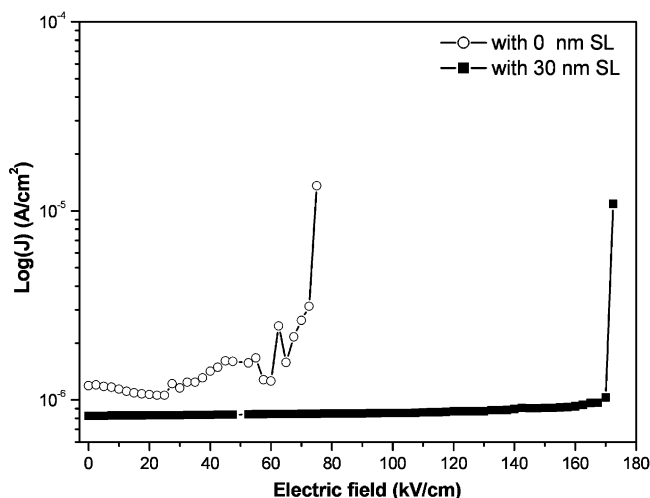

Figure 11. Room-temperature hysteresis loops of $(Ba_{0.8}Sr_{0.2})TiO_3$ films with 0 and 30 nm thick seed layers (SL = seed layer).

cm^2 with a coercive field of 30 kV/cm, which was considerably enhanced when compared to 0.4 $\mu C/cm^2$ for BST films without seed layer. The literature claims for $Ba_{0.8}Sr_{0.2}TiO_3$ sol−gel films and for a well-saturated $P−E$ hysteresis loop a remnant polarization of 3.5 $\mu C/cm^2$ and a coercive field of 53 kV/cm.[17]

Table 1 summarizes the dielectric properties of BST films obtained in this work, in which the effect of the thickness of the seed layer is clearly demonstrated. For comparison, some literature values reported for identical films are also tabulated.

4. Discussion

The above results showed that the insertion of BST seed layers improved the crystallinity and promoted the ($h00$) preferred orientation of BST films deposited by sol−gel on the top of the seed layers at low annealing temperatures (700 °C). Moreover, the obtained results also showed that the effect of the seed layers on the structure and microstructure of BST films is dependent on the thickness of the seed layer, with an optimal thickness existing for the maximization of the degree of texture and, consequently, of the dielectric and ferroelectric properties.

The existence of a seed layer on the bottom of a sol−gel film with an equivalent crystallographic lattice, which nulls the lattice mismatch, can be regarded as a preferential site over which the nucleation of the perovskite phase will easily take place. The thin seed layer of BST will provide the nucleation sites to promote the nucleation (heterogeneous nucleation) and growth of BST films. Hence, in the presence of such a template the nucleation of the perovskite phase will preferentially occur at the top of the seed layer and not in the bulk of the film, and the growth of the crystallites/ grains will occur from the bottom to the top of the film. In this way, the nucleation of BST films will be similar to the nucleation of films grown by physical methods, in which the nucleation of the crystallite phase is confined to islands

Figure 10. Room-temperature current−voltage characteristics of $(Ba_{0.8}Sr_{0.2})TiO_3$ films with 0 and 30 nm thick seed layers (SL = seed layer).

sol−gel derived graded BST films with a tunability of 40% at 230 kV/cm.[16]

Leakage current, a key parameter from the point of view of applications and the effect of the seed layer on the leakage behavior of BST films, is presented in Figure 10. As shown the current density of BST films with an optimal seed layer of 30 nm thick is 8.0×10^{-7} A/cm² up to the applied voltage of 6.7 V (167.5 kV/cm), which was highly improved when compare to 1.2×10^{-6} A/cm² up to 2.6 V measured for BST films without seed layers. The literature reported for sol− gel BST ($Ba_{0.8}Sr_{0.2}TiO_3$) films values of both forward and reverse leakage currents of approximately 1.0×10^{-6} A/cm² up to an applied voltage of 3 V, despite the relatively high dielectric constant of ∼500 at 10 kHz.[16]

Figure 11 depicts the polarization P versus electric field E characteristic of BST films with and without seed layers, measured at 100 Hz and room temperature. Under identical measurement conditions, the $P−E$ hysteresis was improved by the introduction of a seed layer. The remnant polarization P_r of samples with a 30 nm thick seed layer was 1.6 $\mu C/$
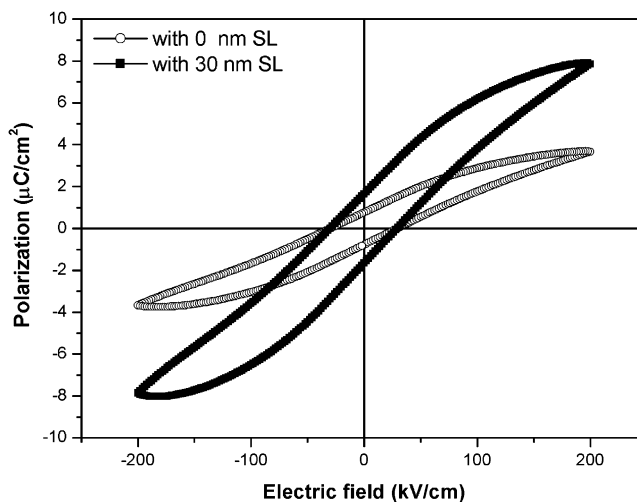
(16) Adikary, S. U.; Chan, H. L. W. *Mater. Chem. Phys.* **2003**, *79*, 157− 160.

(17) Jiang, S.; Zhang, H.; Lin, R.; Liu, S.; Liu, M. *Integr. Ferroelectr.* **2005**, *70*, 1−9.

Table 1. Electric Properties of BST Films Prepared in This Work and Reported in the Literature

Film/T_{ann} (°C)	Deposition Technique	Seed layer/thickness of the film (nm)	ϵ_r (at room temperature)	tan δ	P_r (μC/cm^2)	I (A/cm^2)	Ref
BST(80/20), 700 °C	sol−gel	no seed layer/400 nm	250 (at 1 kHz)	0.03 (at 100 kHz)	0.4	1.2 × 10^{-6} up to 2.6 V	this work
BST(80/20), 700 °C	sol−gel	15/400 nm	320 (at 1 kHz)	0.04 (at 100 kHz)			this work
BST(80/20), 700 °C	sol−gel	30/400 nm	830 (at 1 kHz) or 580 (at 1 MHz)	0.05 (at 100 kHz)	1.6	8.0 × 10^{-7} up to 6.7 V	this work
BST(80/20), 750 °C	sol−gel	no seed layer/260 nm	520 (at 100 kHz)	0.03 (at 100 kHz)	3.5	4 × 10^{-7} at 3 V	16
BST(80/20), 750 °C	sol−gel	sandwich seed layer 40/200 nm	405 (at 10 kHz)	0.011 (at 10 kHz)	2.3		17
BST(70/30), 750 °C	sol−gel	no seed layer/300 nm	400 (at 10 kHz)	0.014 (at 10 kHz)	3	1 × 10^{-6} up to 10 V	24
BST(60/40), 800 °C	sol−gel	no seed layer/160 nm	230 (at 100 kHz)	0.02 (at 100 kHz)		1.6 × 10^{-7} at 3 V	19
BST(70/30)	MOD[a]	no seed layer/300 nm	563			1 × 10^{-6} at 3 V	25[b]

[a] MOD = metalo−organic deposition. [b] Table 1 of ref 25 reports a comparison of some of the best electrical data for BST films prepared by various deposition techniques.

of atoms deposited on the top of the substrate.[18] Moreover, BST films grown on the top of the seed layers will "imitate" the orientation of the seed layers, as it was observed. The (h00) growth direction of BST was favored in the thin seed layer due to the lower crystallization surface energy in this plane than in the other directions (i.e., (101), (111), and (211)). With (h00) preferred orientation seed layers and in identical processing conditions, BST films have, besides the higher degree of crystallinity and bigger grains, a higher degree of texture along the (h00) direction than those non-seeded BST films, as perceived in this work (Figures 1−5). Other authors reported similar results for BST films that were, however, annealed at higher temperatures than those reported here[12,14] and also for other Ba- and Sr-based systems.[6,19]

However, the thickness of the seed layer has a crucial role in the definition of the texture of BST films. Results showed that the (h00) preferred orientation of seeded films is dependent on the degree of orientation of the seed layer, which is by itself dependent on its own thickness. The thickness of the seed layer was shown to control "the location" of the nucleation sites of the crystalline phase. It was observed that above a critical thickness the crystallization of the perovskite phase in the seed layer will be the result of the competing nucleation of the crystalline phase occurring near the top surface of the substrate (the Pt electrode) and in the bulk. In this case the orientation of the seed layer is random. Hence, after that critical thickness which is around 30 nm in the present work, the thicker the seed layer is, the lower the texture degree of this layer will be. Less oriented films were obtained on the top of thick seed layers (Figures 3 and 4).

In agreement with the results here presented it was reported that the success of the seed layer approach in BaTiO$_3$ and SrTiO$_3$ systems requires restricted thickness of the individual layers. Hoffman et al.[20] reported columnar ⟨111⟩ orientated sol−gel SrTiO$_3$ thin films via individual 20 nm thick layers.

According to the authors the individual layer thickness should be restricted to values below the average grain size of equiaxed films. For the preparation of BaTiO$_3$ orientated thin films, Schwartz el al.[6] refer to the use of discontinuous seed layers consisting of small BaTiO$_3$ islands 15−30 nm high and 10−100 nm long. Langjahr et al.[21] reported the preparation of (001) orientated BaZrO$_3$ films when 25−50 nm coatings were used.

As a result of the observed effects of seed layers on the structural and microstructural features of BST films (high degree of crystallinity and texture) an improvement of the dielectric properties of these films is then expected. Indeed, the dielectric and ferroelectric properties of BST films prepared under the current conditions were considerably improved (Figures 8−11). The 400 nm thick sol−gel BST films with an optimal seed layer thickness of 30 nm and annealed at 700 °C have high ϵ_r values of 830 and 600 at 1 kHz and 1 MHz, respectively, which is comparable or even superior to the dielectric properties reported for some BST films prepared by PVD and annealed at higher temperatures (Table 1). This significant improvement of the dielectric constant, also observed in the tunability values when inserting seed layers, is partly attributed to the increase of the grain size and to the (h00) preferred orientation that is believed to lead to an enhancement of the in-plane oriented polar axis,[22,23] which may improve the dielectric response and tunability of BST thin films. The improved tunability of sputtered BST films on Pt/Ti/SiO$_2$/Si was ascribed to the (100) texture of the film leading to an enhancement of the in-plane oriented polar axis.[23] On the other hand, it was also suggested that the seed layer insertion would result in the suppression of the formation of a low dielectric constant interfacial layer between the film and the electrode,[12] ending in improved dielectric properties.[9,22]

Comparing the ϵ_r values at 1 kHz of 830 to 320 and 250 for the 30 and 15 nm thick seed layers and without a seed layer, respectively, it was confirmed that the thickness of

(18) Ren, T.-L.; Wang, X.-N.; Liu, J.-S.; Zhao, H.-J.; Shao, T.-Q.; Liu, L.-T.; Li, Z.-J. *Integr. Ferroelectr.* **2002**, *45*, 13−21.
(19) Ezhilvalavan, S.; Tseng, T.-Y. *Mater. Chem. Phys.* **2000**, *65*, 227−248.
(20) Hoffman, S.; Hasenkox, U.; Waser, R.; Jia, J. L.; Urban, K. *Mater. Res. Soc. Symp. Proc.* **1997**, *474*, 9−16.
(21) Langjahr, A.; Wagner, T.; Ruhle, M.; Lange, F. F. *Mater. Res. Soc. Symp. Proc.* **1996**, *401*, 109−114.
(22) Chang, W.; Kirchefe, S. W.; Pond, J. M.; Horwitz, J. S.; Sengupta, L. *J. Appl. Phys.* **2002**, *92*, 1528−1535.
(23) Taylor, T. R.; Lefevre, M. J.; Nagra, A. S.; York, R. A.; Spec, J. S. *Appl. Phys. Lett.* **1999**, *75*, 3186−3188.

seed layer played also an important role in determining the dielectric response, which is in accordance with the effect of the seed layer thickness observed in the structural and microstructural characteristics of seeded films as previously discussed.

High leakage current is detrimental for application of BST films in the DRAMs device. As shown in Figure 10, the current density changed by 1 order of magnitude, from 1.2×10^{-6} A/cm^2 to 8.0×10^{-7} A/cm^2, when inserting optimized seed layers. Besides reaching the current density value of 8.0×10^{-7} A/cm^2 it can be stable up to an applied voltage of 6.7 V (167.5 kV/cm), followed by a breakdown effect. The low leakage current observed for seeded films is probably caused by the low defect state and absence of a low dielectric interfacial region, which can respond for the low leakage current through BST films. Seed layers can adsorb the planar defects, having the role of a "soft" template as suggested by others.[26]

The improvement of the $P-E$ hysteresis response might be correlated with the large grains and high-preferred orientation along (h00) in seeded films. The P_r value was increased from 0.4 to 1.6 μC/cm^2 for films prepared with the optimal seed layer (Figure 11). The easy movement of the domain walls under an ac field for the case of big grains may affect the increment of the polarization.[26] Moreover, in random BST films the polarizations in different oriented grains possibly will cancel each other, which will decrease

the effective polarization. Indeed, with the increase of (h00) preferred orientation the effective polarization was increased.

5. Conclusion

($Ba_{0.8}Sr_{0.2}$)TiO$_3$ thin films on Pt/Ti/SiO$_2$/Si prepared by sol−gel at 700 °C with (h00) preferred orientation and enhanced dielectric and ferroelectric response were obtained through the use of sol−gel seed layers with optimized thickness. The thickness of 30 nm was observed to be the critical thickness for the seed layer under the present experimental conditions. The seed layer acting as a "soft template" favored the heterogeneous nucleation, enhanced the crystallization of the perovskite phase, restricted the nucleation of the crystalline phase to the bottom layer, favoring textured growth through the (h00) direction, and as a consequence, decreased the defect state of the film. The resultant BST films exhibited improved dielectric, tunability, ferroelectric, and leakage current properties, similar to BST films prepared by physical methods and at high annealing temperatures. The films prepared in this work are suitable for applications in multilayer capacitor technology.

(24) Cheng, G.; Meng, X. J.; Tang, J.; Lou, S. L.; Chu, J. H. *Appl. Phys. A* **2000**, *70*, 411−414.
(25) Velu, G.; Carru, J. C.; Cattan, E.; Remiens, D.; Melique, X.; Lippen, D. *Ferroelectrics* **2003**, *288*, 59−69.
(26) Yi, W.-C.; Kalkur, T. S.; Philofsky, E.; Kammerdiner, L. *Thin Solid Films* **2002**, *402*, 307−310.